Additive manufacturing of patient-specific tubular continuum manipulators

Ernar Amanov, Thien-Dang Nguyen, Jessica Burgner-Kahrs

Ernar Amanov, Thien-Dang Nguyen, Jessica Burgner-Kahrs, "Additive manufacturing of patient-specific tubular continuum manipulators," Proc. SPIE 9415, Medical Imaging 2015: Image-Guided Procedures, Robotic Interventions, and Modeling, 94151P (18 March 2015); doi: 10.1117/12.2081999

SPIE.

Event: SPIE Medical Imaging, 2015, Orlando, Florida, United States

Additive Manufacturing of Patient-Specific Tubular Continuum Manipulators

Ernar Amanov, Thien-Dang Nguyen, Jessica Burgner-Kahrs

Emmy Noether Research Group CROSS,
Center of Mechatronics (MZH), Leibniz Universität Hannover, Hanover, Germany

ABSTRACT

Tubular continuum robots, which are composed of multiple concentric, precurved, elastic tubes, provide more dexterity than traditional surgical instruments at the same diameter. The tubes can be precurved such that the resulting manipulator fulfills surgical task requirements. Up to now the only material used for the component tubes of those manipulators is NiTi, a superelastic shape-memory alloy of nickel and titan. NiTi is a cost-intensive material and fabrication processes are complex, requiring (proprietary) technology, e.g. for shape setting. In this paper, we evaluate component tubes made of 3 different thermoplastic materials (PLA, PCL and nylon) using fused filament fabrication technology (3D printing). This enables quick and cost-effective production of custom, patient-specific continuum manipulators, produced on site on demand.

Stress-strain and deformation characteristics are evaluated experimentally for 16 fabricated tubes of each thermoplastic with diameters and shapes equivalent to those of NiTi tubes. Tubes made of PCL and nylon exhibit properties comparable to those made of NiTi. We further demonstrate a tubular continuum manipulator composed of 3 nylon tubes in a transnasal, transsphenoidal skull base surgery scenario in vitro.

Keywords: Concentric tube continuum robot, fused filament fabrication, additive manfacturing, tubular continuum manipulator, surgical robotics

1. INTRODUCTION

Tubular continuum robots (also referred to as concentric tube continuum robots or active cannulas) have been demonstrated as high potential manipulators for those surgical tasks where a small diameter, flexible, and compliant manipulator is desired. With tube diameters below 3 mm these robots can achieve tentacle-like motion, turn around corners, and maintain high dexterity. The small size allows accessing a surgical site through small incisions or through natural orifices on tortuous paths, such as the nose, ear, or urethra. Various medical applications have been proposed for those continuum manipulators, e.g. neurosurgery,[1] skull base surgery,[2] cardiac surgery,[3] abdominal surgery,[4] or urologic surgery.[5] A tubular continuum robot can either be used as a steerable needle (deployed through tissue) or as a teleoperated manipulator (in cavities of the human body). A review on this continuum robot type can be found here.[6]

Tubular continuum manipulators are composed of multiple, precurved, elastic tubes, which are nested inside of one another (see Figure 1). When telescoping the tubes, i.e. axially rotating and translating each tube at its base, the overall continuous shape of the manipulator changes due to elastic deformation. The workspace, dexterity, workload etc.[7,8] of the manipulator are dependent on the component tubes in terms of their lengths, diameters, wall thicknesss, segmental precurvatures, and material properties. Thus, parameterizing the tubes allows to build diverse tubular continuum manipulators with dedicated characteristics (e.g. using computational tube design algorithms[9]).

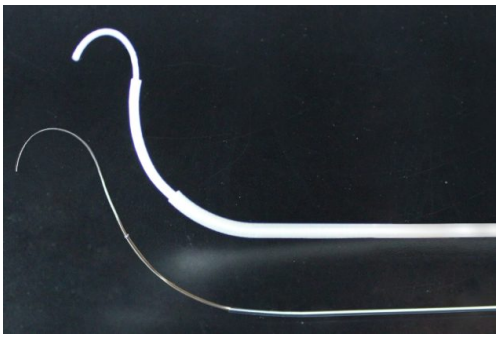

Figure 1. Tubular continuum robot made from NiTi (lower) and thermoplastic (upper).

Corresponding author. E-mail: burgner-kahrs@mzh.uni-hannover.de.

Medical Imaging 2015: Image-Guided Procedures, Robotic Interventions, and Modeling,
edited by Ziv R. Yaniv, Robert J. Webster III, Proc. of SPIE Vol. 9415, 94151P
 · doi: 10.1117/12.2081999

Thus far, component tubes have been fabricated from the shape-memory alloy (SMA) NiTi for two reasons: (1) the shape-memory effect allows prebending the tube into any arbitrary shape and (2) the superelasticity of NiTi in its austenit phase allows tubes to display recoverable strains up to 10 %. The drawback of using NiTi is a relatively high material cost on the one hand and challenges with prebending the tubes on the other hand. The individual tube forming into a desired shape requires a complex heat treatment, which is challenging in terms of the obtainable accuracy of the desired and achieved space curve. The forming process further requires professional equipment of metal working industry. Hence, tubes cannot be produced individually for one specific patient at an instant and availability is dependent on the manufacturer's turnaround time. This makes the general concept of patient- and task-specific tubular continuum manipulators impractical in terms of rapid availability for the surgery.

It would thus be desirable to manufacture component tubes on site right at the hospital in a quick and cost-effective manner with high accuracy and in a sterile environment. We propose to use additive manufacturing technology, as recent efforts have shown feasibility of sterile component fabrication.[10] In this paper, we investigate the feasibility of fabricating elastic tubes for tubular continuum robots using fused filament fabrication with readily available 3D printing hardware. We evaluate the characteristics of 3D printed tubes made from 3 thermoplastics experimentally and proof our concept with a prototype robot.

2. FUSED FILAMENT FABRICATION OF TUBES

2.1 Thermoplastic Materials

Three thermoplastic materials are used for this study: Polyactide (PLA), Polycaprolactone (PCL) (both PLA and PCL from MakerBot Industries, LLC, New York City, NY, USA), and nylon (618, taulman3D, LLC, St. Louis, MO, USA). PLA is a technical biopolymer derived from corn, biocompatible and belongs to the group of polyesther. PCL is a highly elastic material which is similar to polyethylene and can even be reshaped by heating it in hot water. Nylon 618 is a high strength, pliable co-polymer which is biocompatible and resistant to chemical degradation. The melting temperature and nozzle temperature for fused filament fabrication with these materials, as suggested by the manufacturers are listed in Table 1.

The material properties of these 3 thermoplastics differ from NiTi in it austenite phase (see Table 1). PLA and Nylon both possess a high yield strength of 60-70 MPa, while PCL with 16.1 MPa lies well beneath these values. The elasticity modulus of nylon is smaller than the Young's modulus of PLA, while PCL has the lowest value of all three materials. While these are the ideal property values of the thermoplastic materials, the actual material property values after the fused filament fabrication process, which involves heating, melting, and hardening, have to be determined experimentally.

Table 1. Melting and nozzle temperatures for fused-filament fabrication for PLA, PCL, and Nylon as suggested by the material manufacturer. Material properties in comparison to NiTi.

Material	Melting Temperature	Nozzle Temperature	Yield Strength	Young's Modulus
PLA	150 °C	240 °C	60-70 MPa	2.5-7.8 GPa
PCL	60 °C	100 °C	16.1 MPa	0.34-0.36 GPa
Nylon	n.a.	240 °C	60-70 MPa	2-4 GPa
NiTi (austenite)	-	-	195-690 MPa	75-83 GPa

2.2 Fused Filament Fabrication Process

For our initial proof of concept study, we use a 3D printer using fused filament fabrication technology (Replicator 2, Firmware Version 7.6, MakerBot Industries, LLC, New York City, NY, USA). This model allows printing with one material with 11 μm in plane resolution and 100 μm layer resolution within a volume of (28.5 $\times$ 15.3 $\times$ 15.5) cm^3. Filaments (1.75 mm diameter) are extruded through a 0.4 mm nozzle. The nozzle temperature can be set up to 280 °C depending on material properties (see Table 1).

Tubes are modeled using SolidWorks (Dassault Systems, Waltham, MA, USA) and exported as stereolithography files (stl), which were then converted to g-code using the software MakerWare (provided by the manufacturer). Based on our empirical values, tubes are printed in plane and centered on the acrylic printing board.

For PLA and Nylon the printing board is covered with crepe paper tape such that it provides a good adhesion for the filament. In case of PLA it prevents the very strong attachment to the board, which could lead to troublesome separation of the part from the board. PCL filament was printed directly on the board in favor of better adhesion.

We initially fabricated tubes by varying both the printer settings (i.e. layer thickness, infill, and nozzle temperature) and the geometrical tube parameters as a prerequisite for our study. All other printer settings corresponded to the default: 2 shells, 90 mm/s speed while extruding, and 150 mm/s speed while travelling. The layer thickness was set to 0.1 mm, which is the smallest value for this parameter. The infill for tubes is set to 10 %, which empirically led to the best flexibility of the tubes. The nozzle temperature for PLA and nylon was set to 230 °C, while 123 °C was determined best for PCL. We note that these nozzle temperatures vary from those suggested by the manufacturers (compare Table 1).

With these printer settings, we evaluated the minimum tube size which can be printed with acceptable stability and shape by reducing the outer and inner diameters. We were able to fabricate a rod (tube with ID 0 mm) with a diameter of 1.2 mm. Further size reduction led to loss of the tubular shape as edges of the layers became apparent. As a result, the minimum wall thickness of tubes was defined as 0.6 mm. Fabrication times varied by the amount of filament from 3-10 min, which is dependent on the tube diameter, wall thickness, and length.

2.3 Tubes Fabrication

For our study, we consider component tubes with an initial straight section with length L_s followed by a section of constant curvature κ with length L_c. The tubes are further defined the inner (ID) and outer diameter (OD). As the variation of all 5 parameters would result in a diverse amount of tubes, we focus on two parameters which influence the flexibility: OD and κ. By variation of these 2 parameters we can determine boundaries of the thermoplastic materials in terms of how elastic the tubes are after printing. Thus, the other parameters are set to constant values (see Table 2).

Table 2. Tube parameters with the variation of ID, OD, and curvature.

Tube No.	L_s[mm]	L_c[mm]	κ[mm^{-1}]	ID[mm]	OD[mm]
1	100	40	1/15	0	1.2
2			1/30		
3			1/50		
4			1/90		
5	100	40	1/15	0.8	2
6			1/30		
7			1/50		
8			1/90		
9	100	40	1/15	1.8	3
10			1/30		
11			1/50		
12			1/90		
13	100	40	1/15	2.8	4
14			1/30		
15			1/50		
16			1/90		

L_s is chosen to correspond with the length of the translational axis of the robot's actuation unit used for this study (see Section 3.2). The inner diameter was chosen by the most thinnest possible wall thickness (0.6 mm, compare Section 2.2). Thus, the inner diameter is chosen to be 1.2 mm smaller than the outer diameter. We evaluate four different outer tube diameters with the same wall thickness of 0.6 mm and four different curvatures with the same length L_c of 40 mm for all tubes. The length of the curved section 40 mm, maximum outer diameter 4 mm, and curvatures were chosen as they are considered sufficient in regard of the application field

in confined spaces in the human body such as the nose.[2] This results in 16 tubes fabricated for each material. Figure 2 shows the printed tube sets from PLA numbered according to Table 2.

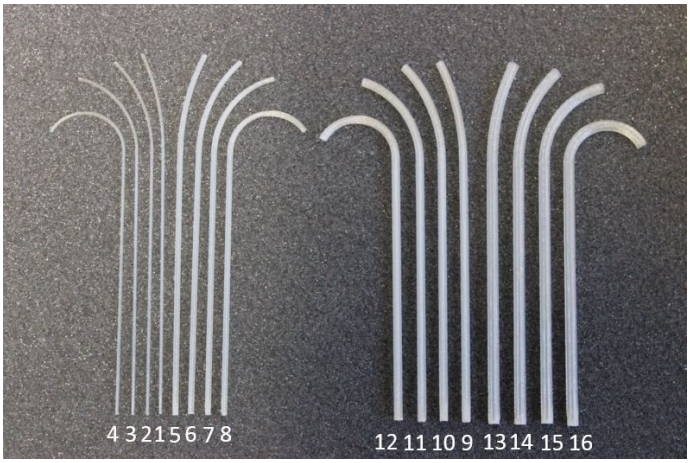

Figure 2. Fabricated PLA tubes.

3. THERMOPLASTIC TUBES PROPERTIES INVESTIGATION

3.1 Tension Testing

The manufacturer provides data about the materials mechanical properties: Young's modulus and yield strength (see Table 1). However, these values can change after the printing procedure due to the temperature treatment and the attachment forces between the material layers. Hence, we determine these materials characteristics after $3D-$printing by performing a tension test. Figure 3 shows the experimental setup. A material sample is fixed at the bottom to a solid board and at the top to a force/torque sensor (ATI Mini40, ATI Industrial Automation, Apex, NC, USA). By rotating the crank a tension force is applied to the sample. The force/torque sensor's axial force range is 240 N and axial accuracy 0,04 N. At the same time the axial distance is measured using a range sensor (WA10, Hottinger Baldwin Messtechnik GmbH, Darmstadt, Germany) with a maximum range of 10 mm and accuracy of 1 °. This distance is equivalent to the elongation of the material. The force is applied until the sample breaks apart or is visibly not intact anymore. Yield strength and Young's modulus can then be determined from the measured data. The yield strength is considered to be the maximum tension and the Young's modulus is the slope between the elongation of zero and 0.5 %, which is the area where the Hooke's law is effective.

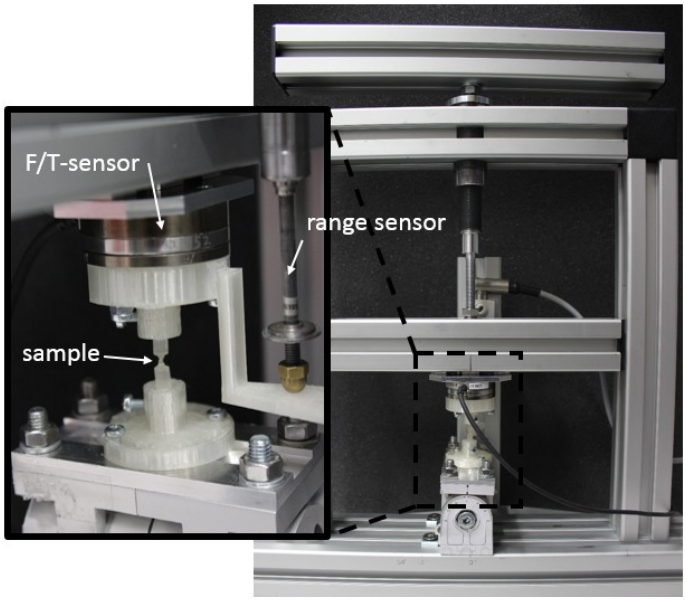

Figure 3. Experimental setup for tension testing. A material sample is mounted to a F/T sensor. A range sensor measures the elongation of the sample until breaking.

We performed tension testing for all three thermoplastics. For each material 5 samples with a minimum diameter of 1 mm were fabricated and evaluated. These samples were printed with the same printer settings as outlined in Section 2.2, but with 100 % infill in order to be able to calculate the tension. The resulting measurement data is fitted by a polynomial curve in order to dismiss the noise and external influences on the set up, e.g. force through

the rotation of the crank. Only the force in the direction of pulling was considered since the other forces were significantly small (below 0.5 N).

Figure 4(left) shows 5 measurements of PLA samples. Although the maximum stress varies between 31-48 MPa, the linear behavior is clearly similar and recognizable. Its values vary between 4.7-5.1 GPa. Same behavior can be observed for the other two materials. For PCL the linear section is 0.05 % shorter than for nylon and PLA. Table 3 summarizes the experimentally obtained yield strength and Young's modulus for all materials.

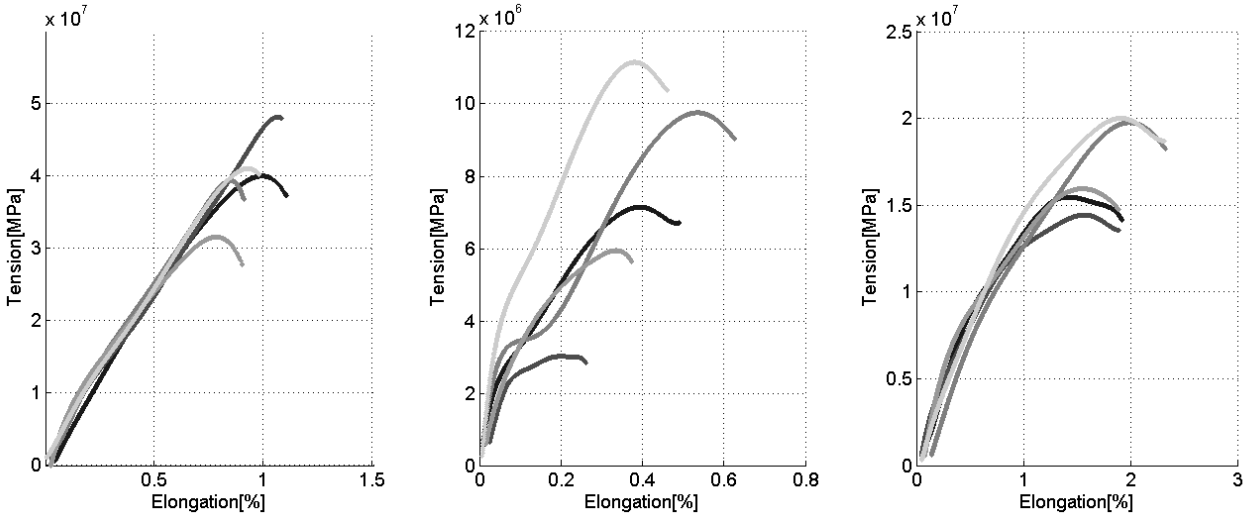

Figure 4. Stress-Strain Diagram with 5 measurements for PLA (left), PCL (middle), nylon (right)

Table 3. Yield strength and Young's modulus for PLA, PCL, and Nylon.

Material	Yield Strength (Mean) [MPa]	Young's modulus (Mean) [GPa]
PLA	31-48 (40)	4.7-5.1 (4.9)
PCL	3-11.1 (7.4)	1.4-3.8 (2.4)
Nylon	14.4-20 (17.1)	1.44-1.97 (1.73)

3.2 Tube Actuation Unit

In order to evaluate the properties of the fabricated tubes under translational and rotational actuation, we built a semi-manual actuation unit (see Figure 5a). Tubes are mounted to carriers sliding on a rail along individual lead screws. Each carrier features a collet for quick exchange of component tubes. Translation is achieved by DC motors connected with their shaft to each lead screw. Axial rotation of each tube can be manually controlled by turning a knob on each carrier. The actuation unit was mostly build from fused filament fabricated parts, except mechanical parts for actuation.

3.3 Deformation Properties

We determine the flexibility of thermoplastic tubes by evaluating the degree of plastic deformation. A straight, stiff outer tube is fabricated from PLA (OD 8 mm and ID $\in$ [2,2 mm, 3 mm, 4 mm, 5 mm] depending on inner tube OD), mounted to the actuation unit (see Section 3.2), and pushed out by the length of the curved section (40 mm). Each fabricated tube (see Table 2) is then nested inside a straight outer tube and mounted to the actuation unit's middle carrier, such that its curved section is extended beyond the tip of the outer tube (referred to as initial position in the following, see Figure 5b(1)). The examined tube is then pulled back into the outer tube until both tips align and pushed out again for the same distance (Figure 5b(2)). This procedure is repeated 5 times for each tube. The initial tip position and tip position after each pull/push sequence are measured using a measurement arm (Faro Gage, FARO Europe GmbH & Co. KG, Korntal-Münchingen, Deutschland).

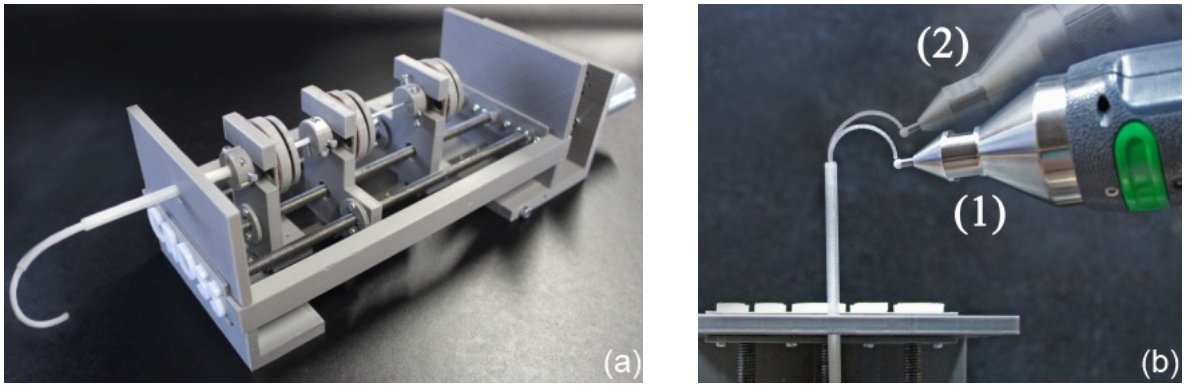

Figure 5. (a) Actuation unit for component tubes made from thermoplastics. (b) Experimental evaluation of tube deformation properties by measuring tip error before (1) and after translation (2).

The distance between the first tip position and the following measurements is the error which is determined for all 5 repetitions. The mean deformation error is summarized in Table 4 for all three materials. PLA tubes with a diameter of 4 mm and some with 3 mm were too stiff to be pulled in, as were some tubes made of Nylon and PCL. Those tubes are marked with an x in Table 4. Tubes made from PLA resulted in a tip error in the range of 0.3-3.1 mm. In comparison, the mean tip error range using nylon tubes was 0.4-7.6 mm and PCL tubes was 0.2-9.8 mm. We observed that the tip error rises with the diameter and the curvature. For comparison, the same experiment is performed using a tube made of NiTi (OD 1.2 mm, ID 0.88 mm, κ 1/30 mm^{-1}, L_c 40 mm). The comparison study with NiTi tubes resulted in a mean error of 1.49 mm.

Table 4. Mean tip position error (in mm) due to plastic deformation. x indicates that the tubes could not be evaluated.

Tube No.	1	2	3	4	5	6	7	8	9	10	11	12	13	14	15	16
PLA	0.31	0.5	0.4	3.1	0.3	0.9	1.2	x	0.3	1.1	x	x	x	x	x	x
PCL	0.2	0.25	1.27	1.96	0.62	0.9	1	6.1	0.8	1.5	2.5	9.8	1.5	3.2	x	x
Nylon	0.4	0.7	1.2	1.8	0.55	0.5	1.2	6.1	0.75	1.2	4.9	7.6	1.9	1.4	x	x

3.4 Accuracy of Manipulator Composed of Thermoplastic Tubes

With this experiment, we evaluate the absolute positioning accuracy of Nylon tubes as their surface is the smoothest among all materials. In order to measure the impact of plastic deformation to the tubes, we use two tubes (No. 6 and No. 15 from Section 2) and an outer straight tube with OD of 6 mm and ID of 4.8 mm. Those tubes were mounted to the actuation unit (Section 3.2). We evaluate the accuracy at 15 randomly generated robot configurations. The geometrically exact kinematic model[11] was used to calculate the theoretical position of the inner tube tip for each configuration and compared to the position achieved with the robot. Measurements were taken using the measurement arm.

The spatial distribution of the measurement is illustrated in Figure 6 where dots correspond to the theoretical tip position obtained with the kinematic model and measured points are indicated by a cross. The black area corresponds to the approximate workspace of the robot. The error ranged between 1.13-6.9 mm with a mean error over all 15 measurements of 3.7 mm. This error is comparable to the error reported for NiTi tubes.[11]

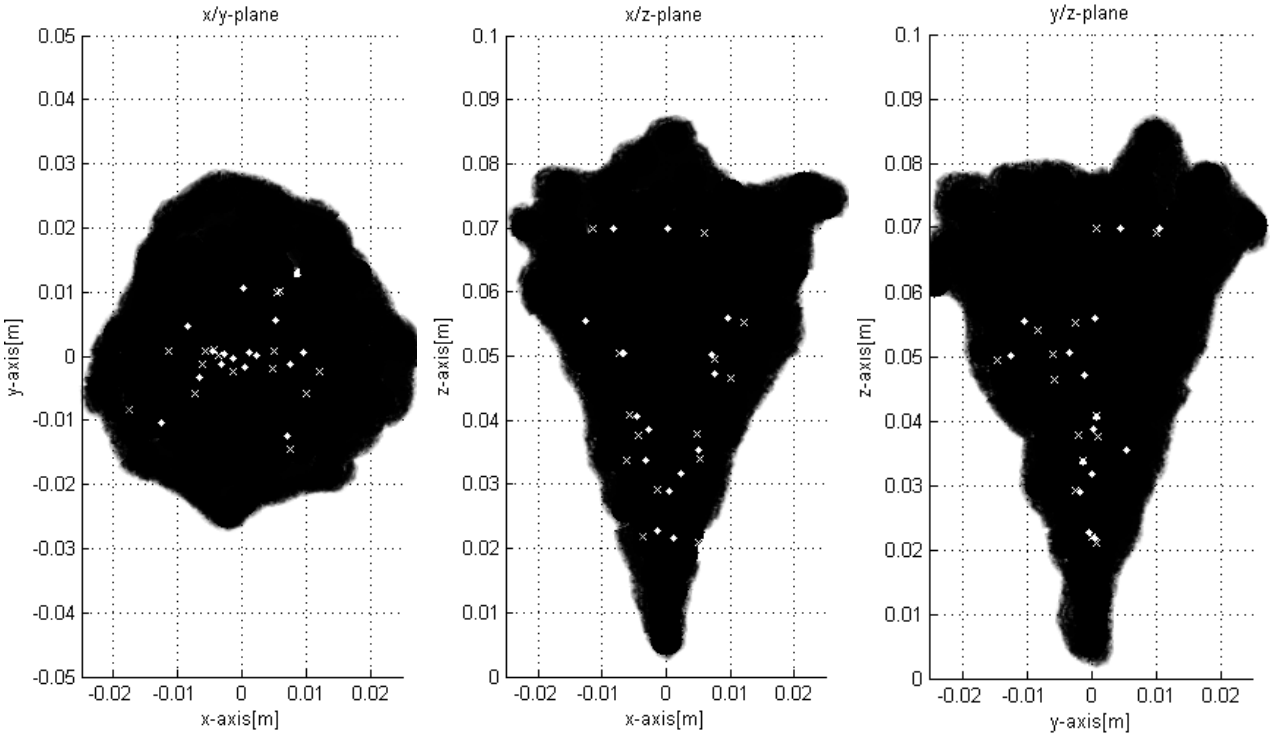

Figure 6. Model tip positions (dots) and measured tip positions (cross) for accuracy experiment using nylon tubes in the x-/y-, x-/z-, and y-/z-plane. The black area marks the approximate workspace of the manipulator.

4. DISCUSSION

Additive manufacturing of tubes using fused filament fabrication is feasible. The key towards optimal results in fabrication is the determination of printer settings. For our study, we have seen that the nozzle temperature is an important factor for the tube properties. The calibration of the printer, in particular the distance between the printing board and the nozzle, turned out a crucial step for printing the first layer and obtaining optimal adhesion. In terms of the tube's surface properties, we rank PLA the worst. The surface of the tubes is not smooth which leads to higher friction when assembled to a tubular continuum robot. PCL tubes have better surface properties, but nylon tubes exhibit the smoothest surface. The clearance between two nested tubes is set to 0.4 mm for the fabricated tubes as they exhibit higher friction. We note that for this study, we did not post-process the surface of the fabricated tubes. The minimum obtainable wall thickness's of 0.6 mm restricts the miniaturization of tubes. A 3D printer with higher resolution and lower layer thickness could be used to improve on this.

As the fused filament fabrication melts the material and applies it in layers, the material properties such as yield strength and Young's modulus can vary significantly from those of the unextruded material. Young's modulus is in particular important, as it is a parameter required within the kinematic model and influences the model accuracy. Our tension experiment revealed that the yield strength varies from sample to sample. We suspect that this is caused by the area which cannot be defined explicitly for the printed tubes. It would thus be beneficial to further analyze the printing process and evaluate the influencing parameters.

The deformation of the three tube materials, as reported in Section 3.3, is neglectable for tubes made from nylon and PCL for small tube outer diameters. We have observed that PLA soon becomes too stiff as tubes could not be inserted into the outer tube. However, the results for ODs $\leq$2 mm compare with those for nylon and PCL. Tubes with high curvatures showed larger deformation in comparison to those with smaller curvature. We note, that these were short-term deformation experiments (inner tuber remained within outer tube for a few seconds). The influence of long term deformation should be evaluated. We have empirically observed that nylon and PCL tubes recovered their initial curvatures over short amounts of time. However,

we did not evaluate this any further in the scope of this paper.

Our accuracy study of a tubular manipulator with nylon tubes resulted in comparable errors to those obtained with NiTi tubes. We note, that our tubes were significantly shorter as those reported in the literature. Shorter tubes are known to results in lower errors.[11]

As a proof of concept, we used a tubular manipulator made of 3 nylon component tubes (straight outer tube, middle tube No. 9, inner tube No. 4, see Table 2). The actuation unit depicted in Figure 5a was used to deploy the manipulator through the nasal cavity of an anatomical model (cross section of human skull, 3B Scientific, Hamburg, Germany). We were able to reach the skull base on a transnasal, transsphenoidal path (see Figure 7). This approach allows surgical removal of tuberculum sellae meningiomas or pituitary tumors minimally-invasively.[2]

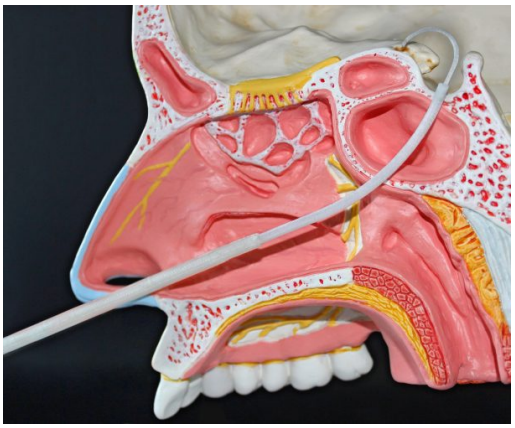

Figure 7. Reaching the skull base on a transnasal, transsphenoidal path with a manipulator made of nylon tubes.

5. CONCLUSION AND OUTLOOK

We have shown principal feasibility of fabricating component tubes for tubular continuum manipulators using additive manufacturing using an off-the-shelf 3D printer. Tubes made from PLA did not exhibit the elasticity properties needed for concentric tube manipulators. In contrast, tubes fabricated from nylon and PCL have low friction surfaces and exhibit properties comparable to NiTi.

We evaluated the properties of thermoplastic tubes made with fused filament fabrication in a series of experiment. This is a first step towards more rigorous evaluations, e.g. long term deformation, influence of printer settings, and post processing of tube surface to decrease friction.

In terms of on site tube fabrication in a sterile environment, an FDA approved nylon (Taulman 680 and 910) is currently under certification. In combination with the advancements in sterile additive manufacturing technology,[10] our method will enable custom, patient-specific continuum manipulators, produced on-demand. We expect that the low production cost and time efficiency can potentially add therapeutic value.

ACKNOWLEDGMENTS

This work was funded by the Emmy Noether Programme of the German Research Foundation (DFG) under award number BU 2935/1-1. The authors thank the Institute of Mechatronic Systems at Leibniz Universitat Hannover, in particular Jan-Philipp Kobler, for providing us with the test bench for the tension tests.

REFERENCES

[1] Burgner, J., Swaney, P. J., Lathrop, R. A., Weaver, K. D., and Webster III, R. J., "Debulking from within: a robotic steerable cannula for intracerebral hemorrhage evacuation.," *IEEE Trans Biomed Eng* **60**(9), 2567–75 (2013).

[2] Burgner, J., Rucker, D. C., Gilbert, H. B., Swaney, P. J., Russell, P. T., Weaver, K. D., and Webster III, R. J., "A Telerobotic System for Transnasal Surgery," *IEEE/ASME Trans Mech* **19**(3), 996–1006 (2014).

[3] Gosline, A. H., Vasilyev, N. V., Butler, E. J., Folk, C., Cohen, A., Chen, R., Lang, N., Del Nido, P. J., and Dupont, P. E., "Percutaneous intracardiac beating-heart surgery using metal MEMS tissue approximation tools.," *J Robot Res* **31**(9), 1081–1093 (2012).

[4] Burgner, J., Swaney, P. J., Bruns, T. L., Clark, M. S., Rucker, D. C., Burdette, E. C., and Webster III, R. J., "An Autoclavable Steerable Cannula Manual Deployment Device: Design and Accuracy Analysis," *J Med Device* **6**(4), 041007 (2012).

[5] Hendrick, R. J., Herrell, S. D., and Webster III, R. J., "A Multi-Arm Hand-Held Robotic System for Transurethral Laser Prostate Surgery," in *IEEE Int Conf Robot Autom*, 2850–2855 (2014).

[6] Gilbert, H. B., Rucker, D. C., and Webster III, R. J., "Concentric Tube Robots: The State of the Art and Future Directions," in *Int Symp Robot Res*, (2013).

[7] Granna, J. and Burgner, J., "Characterizing the Workspace of Concentric Tube Continuum Robots," in *45th Int Symp Robot*, 730–736 (2014).

[8] Burgner-Kahrs, J., Gilbert, H. B., Granna, J., Swaney, P. J., and Webster, III, R. J., "Workspace Characterization for Concentric Tube Continuum Robots," in *IEEE/RSJ Int Conf Intell Robot Syst*, 1269–1275 (2014).

[9] Burgner, J., Gilbert, H. B., and Webster III, R. J., "On the Computational Design of Concentric Tube Robots: Incorporating Volume-Based Objectives," in *IEEE Int Conf Robot Autom*, 1185–1190 (2013).

[10] Rankin, T. M., Giovinco, N. a., Cucher, D. J., Watts, G., Hurwitz, B., and Armstrong, D. G., "Three-dimensional printing surgical instruments: are we there yet?," *J Surg Res* **189**(2), 193–7 (2014).

[11] Rucker, D. C., Jones, B. A., and Webster III, R. J., "A Geometrically Exact Model for Externally Loaded Concentric-Tube Continuum Robots," *IEEE Trans Robot* **26**(5), 769–780 (2010).